

The Lorentz factor for basal reflections from micaceous minerals in oriented powder aggregates

R. C. REYNOLDS, JR.

*Department of Earth Sciences, Dartmouth College
Hanover, New Hampshire 03755*

Abstract

A mathematical analysis is made of the Lorentz factor that applies to partially oriented powder aggregates, analyzed by means of the flat-specimen X-ray diffractometer. Equations are derived that include the effects of preferred orientation on absolute and relative intensities. Consideration is given to the Lorentz, geometric, and powder ring distribution factors, collectively referred to here as the Lorentz factor. Calculated results show that preferred orientation must be extreme in order to obtain significant departures from the random powder form of the Lorentz factor, and experimental data on clays indicate that glass slide and porous plate techniques do not produce such high degrees of preferred orientation. If a fine Soller slit (or a graphite monochromator) is used, the application of the random powder Lorentz factor will result in no significant errors for such samples.

Introduction

The flat-specimen X-ray diffractometer has been widely adopted since its development in the 1950s. It has largely replaced the various powder diffraction camera techniques and is now one of the most useful analytical devices in the field of clay mineralogy. Despite its popularity there has been, to the writer's knowledge, no rigorous analysis of the mathematical form of the Lorentz factor that applies to the flat-specimen diffraction geometry. The purpose of this communication is to accomplish such an analysis for partially oriented micaceous aggregates.

Reynolds (1965, 1967, 1969) and Reynolds and Hower (1970) have argued that the random powder Lorentz factor should be applied, even for highly oriented specimens. Good agreement between observed and calculated diffraction intensities was achieved when the random powder version was used. But the writer has received some objections to the acceptance of this conclusion, based as it is on empirical evidence alone. The argument is not trivial; errors of a factor of ten or more will result if the inappropriate form of the Lorentz factor is applied to intensities at the lowest 2θ ranges for peaks from common clay minerals, for example, the glycol-smectite 001.

Diffraction geometry and the Lorentz factor

The derivation here is similar to the standard form followed by many textbooks on the subject. The reader is referred, for example, to James (1965, p. 47). But the mathematical description given below includes a consideration of the flat-specimen diffractometer geometry, and of partially oriented powder aggregates.

In Figure 1 the arrow coincident with the diameter $A-D$ depicts the incident and undeviated X-ray beam that passes through a sample (S) located at the center of a sphere whose radius equals the diffractometer radius (r_0). A normal to the sample surface penetrates the sphere at B and one-quarter of the detector slit is located at C . The angle between the incident (or diffracted) beam and the sample surface is θ , and for any value of θ , the slit is located at the angular position 2θ and the sample normal is at $90-\theta$.

Measurable diffraction effects are limited to reflecting planes whose normals penetrate the surface of the hemisphere of base $A-D$. If the sample consists of a randomly oriented powder, these normals will produce a uniform distribution of pole penetrations over the hemisphere. All planes so oriented as to reflect into the diffraction arc p have normals that are distributed along the arc q , or are located within a small

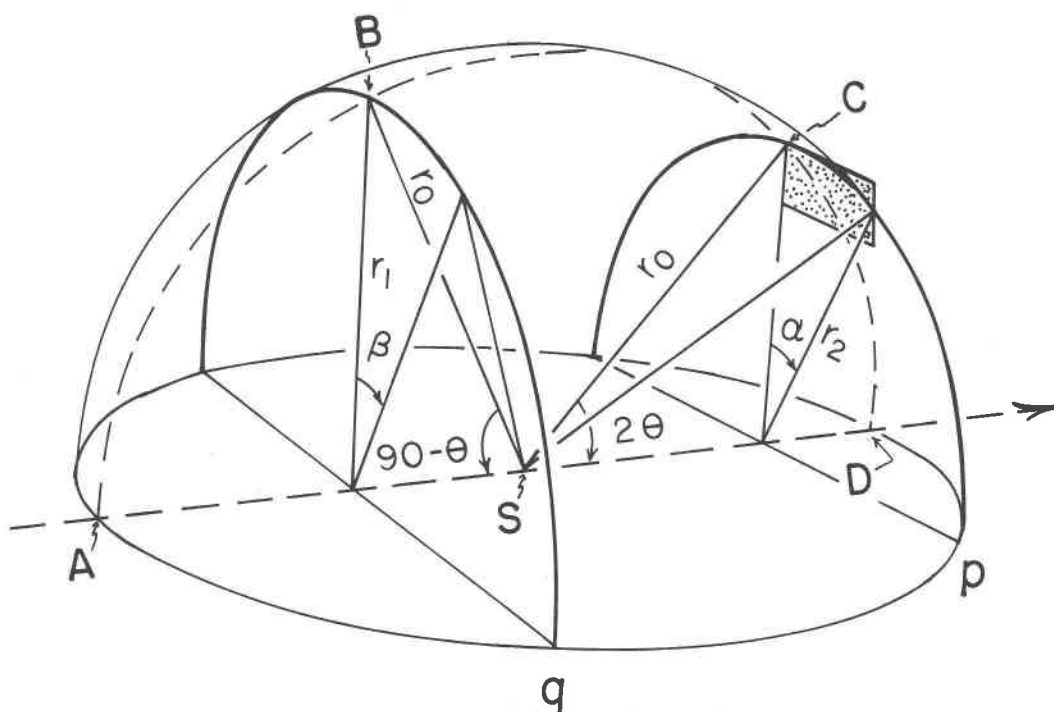


FIG. 1. Geometry of sample, diffractometer, and powder diffraction rings.

distance on either side of q . The distance $\Delta\theta$ is very small, of the order of a few minutes of arc, and it does not change with respect to θ . The area of the critical zone along arc q is its length times $2\Delta\theta$, and the length is $2\pi r_1/2$ where $r_1 = r_0 \sin(90-\theta)$. The area is thus $r_0 \cos\theta \cdot 2\Delta\theta$, and the fraction of crystallites so oriented as to diffract into p is $\pi r_0 \cos\theta \cdot 2\Delta\theta / 2\pi r_0^2$, or $\cos\theta \cdot 2\Delta\theta / 2r_0$. The quantities r_0 and $\Delta 2\theta$ are constant, consequently the fraction of crystallites contributing to the diffraction halo p is proportional to $\cos\theta$.

An intensity measurement at C involves only a small segment of the arc p , whether the detection aperture is a goniometer slit or the slit of a densitometer that is used to record densities from the film of a powder camera. We must, therefore, calculate the fraction of the total intensity that is diffracted into a small length of arc that is enclosed by the slit length $l/2$ ¹. The total length of arc p is πr_2 where $r_2 = r_0 \sin 2\theta$, and thus the fraction of the arc entering is $l/2 / \pi r_0 \sin 2\theta$. Now, l , π , and r_0 are constant, consequently the measured intensities will change proportionately to $1/\sin 2\theta$. This must be multiplied by

$\cos\theta$, derived above, and we have $\cos\theta / \sin 2\theta = 1/\sin\theta$.

Any crystallite or volume element of a crystallite shows a diminution of diffraction intensities proportional to $1/\sin 2\theta$. This factor is related to the change in the irradiated area of a crystal volume element as the diffraction angle is varied (James, 1965, p. 41). By itself, it constitutes the single crystal Lorentz factor. But for a powder aggregate it must be multiplied by $1/\sin\theta$, derived above, and we have

$$(1) \quad L = \frac{1}{\sin 2\theta \sin \theta},$$

the random powder Lorentz factor.

The Lorentz factor when the slit height is small

On the basis of this background, we now consider the behavior of a partially oriented powder aggregate. The treatment is based on the following assumptions.

- (1) The orientation of the particles is described by a Gaussian distribution function, $e^{-k^2\epsilon^2}$, where ϵ denotes the angular departure in degrees from the mean position of all poles that are normal to the basal diffracting planes of the

¹ One-half of the diffraction geometry is considered here because, by symmetry, the other half is identical.

crystallites, and $\kappa = 1/\sqrt{2S}$ where S is the standard deviation of the normals about the mean.

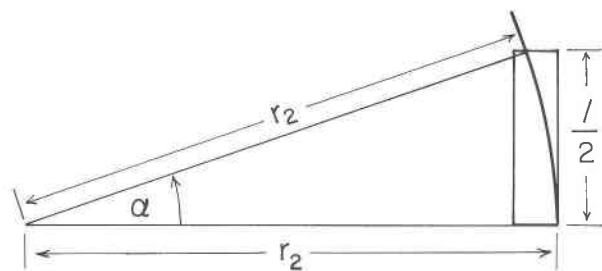
- (2) The mean pole position is defined by a line that is normal to the sample surface.
- (3) The distribution function is circularly symmetrical, that is, the particle distribution has no lineation.

On Figure 1, such a distribution can be diagrammatically described by a series of circular contours centered on B . These have been omitted from the figure in order to preserve its clarity with respect to the other features shown, but the reader should keep this condition in mind during the derivation given below.

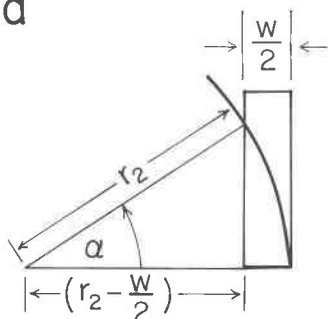
The measured intensity at 2θ (Fig. 1) is given by summing the Gaussian distribution function over the limits zero to $l/2$, where l is the length of the detector slit. Only crystallites so oriented as to diffract into l contribute to the diffraction intensity, and the proportion of these varies with θ and with κ . The angle α in arc p is fixed by the slit.

$$r_2 = r_0 \sin 2\theta, \quad \text{and} \quad \alpha = \sin^{-1} \left(\frac{l}{2r_0 \sin 2\theta} \right)$$

(Fig. 2a). Evidently, α in arc p is equal to β in arc q , consequently we must sum the Gaussian distribution



a



b

FIG. 2. Powder ring limitation by (a) slit-length, and (b) slit-width. Label nomenclature is the same as that of Fig 1.

surface over a range that corresponds to β on arc q . But the angular range β on arc q is not equal to the angular range ϵ for the distribution function because r_1 , the radius of q , is smaller than r_0 which is the radius of the Gaussian surface. Consequently we must multiply α by r_1/r_0 . Now, $r_1 = r_0 \sin(90-\theta) = r_0 \cos\theta$, and $r_0 \cos\theta/r_0 = \cos\theta$. Thus the limit of integration in ϵ , defined here as a , is

$$(2) \quad a = \cos \theta \sin^{-1} \left[\frac{l}{2r_0 \sin 2\theta} \right].$$

Figure 2b shows the consequence of long slit lengths and/or low values of 2θ . Then, the extent of the powder ring admitted by the slit becomes slit-width limited rather than slit-length limited. The limit a in (2) is then

$$(3) \quad a = \cos \theta \cos^{-1} \left[\frac{r_0 \sin 2\theta - w/2}{r_0 \sin 2\theta} \right]$$

where w is the slit-width in centimeters. The selection of the appropriate limit is easily made. The correct value is always the smaller of the two values for a .

One-half the number of crystallites so oriented as to diffract into the slit is given by

$$(4) \quad n = c \cdot 2 \Delta\theta \sum_{\epsilon=0}^{\epsilon=a} e^{-\kappa^2 \epsilon^2} \Delta\epsilon,$$

where c and $\Delta\theta$ are constants. For any real application, relative values for n are required, values that correctly describe the intensities of diffraction peaks from a given mineral at different values of θ . Hence, we always consider a ratio of the quantities n , and c and $2\Delta\theta$ both cancel for such an operation. The Lorentz factor can then be written;

$$(5) \quad L = \sum_{\epsilon=0}^{\epsilon=a} e^{-\kappa^2 \epsilon^2} \Delta\epsilon \cdot \frac{1}{\sin 2\theta}.$$

Suppose that Equation 5 is applied to a single crystal. Then, all "crystallites" are in a position to diffract at all Bragg angles of θ because the distribution function is narrow compared to the slit length. In short, increasing a from its value in (2) to ∞ causes no change in the value of the summation. The summation then yields a constant value for all values of θ and we have the single crystal Lorentz factor,

$$L \propto \frac{1}{\sin 2\theta}.$$

Consider now the random powder condition. This is equivalent to making κ very small (standard deviation very large). If κ is so small that all values of $e^{-\kappa^2 \epsilon^2}$ are close to unity, then the value of the summation in

(5) approaches simply the limit given by (2). If the length of the receiving slit is very small compared to the goniometer radius, r_0 , then the angle α (Figure 1) is very small. For small angles, α is proportional to $\sin\alpha$, so

$$\sin^{-1} \frac{l}{2r_0 \sin 2\theta} \propto \frac{1}{\sin 2\theta}.$$

Multiplying by $\cos\theta$ gives $\cos\theta/\sin 2\theta = 1/\sin\theta$, and multiplying by the single crystal factor provides the final form of the Lorentz factor, *i.e.*

$$L \propto \frac{1}{\sin 2\theta \sin^2 \theta},$$

and this is the random powder form. Thus we see that applying the proper limiting conditions to (5) results in the appropriate forms of the Lorentz factors.

The Lorentz factor: general solution

The effective length l of the receiving slit, treated by (2), is not controlled by the slit itself. Rather, the length is fixed by the separation of the plates in the detector Soller slit assembly. Each Soller slit space defines a slit of minute length. If there are, say, ten such increments in a typical Soller slit, then the sample surface is viewed by the detector in ten small, identical, increments. For our purposes it is necessary only to solve for the radiation transmitted by one such cell, as a function of 2θ .

Unfortunately, Soller slit assemblies in common use allow horizontal divergences² that correspond to relatively large effective values of l (2). Then, the length l can no longer be considered very small compared to the goniometer radius, and (5) is not valid unless l is very small. But the difficulty is overcome by summing (5) over the slit area. The procedure detracts from the simplicity of the derivation, but it is necessary for accurate results if medium resolution Soller slits are used. For fine Soller slits (horizontal divergence $<0.5^\circ$) and probably for goniometers equipped with crystal monochromators, the simpler form of (5) will suffice for most work.

Summation of the powder arcs over the horizontal range of the slit can be visualized by the aid of Figures 1 and 3. The slit is considered to be fixed in space, and the spherical geometry containing the sample and powder rings is moved in small successive increments D (Figure 3) in a direction parallel to the

slit length. The summation is continued until limited by the divergence, that is, until a powder increment is displaced from the slit center by an amount so large that no portion of its powder ring is transmitted to the detector.

Figure 3 shows that two different geometrical configurations are involved. One, Figure 3a, occurs when an increment of powder P is displaced from the slit axis (dashed line) by an amount D where D is less than $S_0/2$; the latter signifying one-half the spacing of the plates in the Soller slit. The other configuration results when $D > S_0/2$ (Figure 3b). Thus it is convenient to break the summation into two parts, so that

$$(6) \quad n = \sum_0^{S_0/2} \sum_{-a_1}^{a_2} e^{-\kappa^2 \epsilon^2} \Delta\epsilon \Delta D + \sum_{S_0/2}^{D_1} \sum_{-b_1}^{-b_2} \Delta\epsilon \Delta D.$$

The limit D_1 can be calculated from the geometric restrictions shown by Figure 3, and it is given as

$$D_1 = \frac{S_0(Y + 2Z)}{2Y}.$$

The summations are taken over one-half the possible values of D , but over the entire slit length. The quantities X , Y , and Z (Figure 3) denote the following. X is the distance from the center of the detector slit to the outer edge of the Soller plates, Y is the length of the Soller plates, and Z is the distance from the inner edge of the plates to the center of the sample. $X + Y + Z = r_0$, the goniometer radius.

The limits a_1 and a_2 are also derived from the geometry shown by Figure 3. The derivation is tedious but not conceptually difficult, and is not presented here. The interested reader can derive it himself with the aid of Figure 3. The quantities l_1 and l_2 in Figure 3 are identical with l in (2), but because summation is taken over the entire slit length, the two in the denominator is eliminated and we have

$$a_{1,2} = \cos \theta \sin^{-1} \left(\frac{l_{1,2}}{r_0 \sin 2\theta} \right).$$

Appropriate limits are:

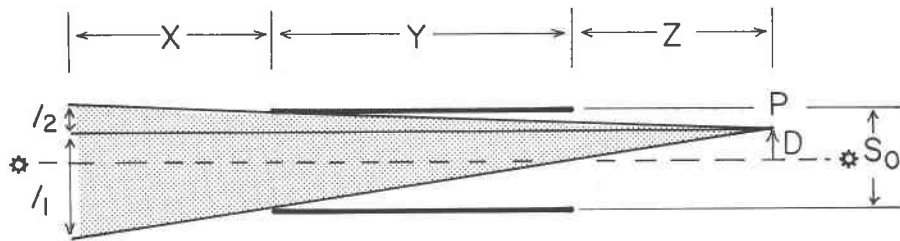
$$a_1 = \cos \theta \sin^{-1} \left(\frac{S_0 + 2D}{2(Z + Y) \sin 2\theta} \right),$$

$$a_2 = \cos \theta \sin^{-1} \left(\frac{S_0 - 2D}{2(Z + Y) \sin 2\theta} \right),$$

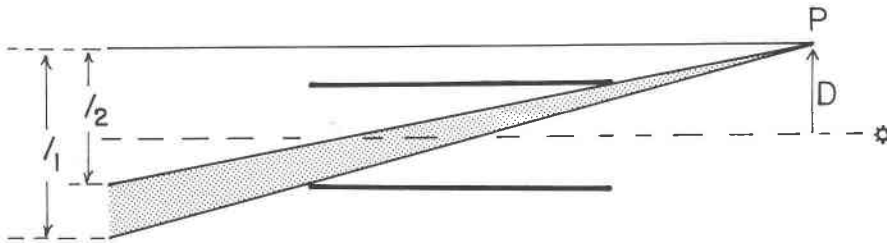
$$b_1 = \cos \theta \sin^{-1} \left(\frac{S_0 + 2D}{2(Z + Y) \sin 2\theta} \right), \quad \text{and}$$

$$b_2 = \cos \theta \sin^{-1} \left(\frac{2D - S_0}{2Z \sin 2\theta} \right).$$

² The terminology here and elsewhere in this paper is consistent with the geometry of Figure 1. Horizontal divergence denotes horizontal divergence from a horizontal sample surface.



a



b

FIG. 3. Soller slit control of the limits of summation in Equation 6.

As before, each step in the summation must be checked for the appearance of the slit-width limiting condition, and when this occurs, the appropriate values for a_1 , a_2 , b_1 , or b_2 are given by (3).

Comparison of intensities between two minerals

The relative change in peak height with respect to 2θ will be correctly given by (7), which contains the powder ring distribution factors, the polarization factor, and the crystal volume element Lorentz factor, *viz.*

$$(7) \quad LP = \frac{n(1 + \cos^2 2\theta)}{\sin 2\theta},$$

when n is a solution of (6).

If quantitative analysis is attempted by means of peak height measurements of two peaks, each from a different mineral species which has a different orientation factor, κ , (7) for a given species is normalized by dividing by

$$\sum_0^{90} e^{-\kappa^2 \epsilon^2} \Delta \epsilon.$$

The procedure provides a value for the number of crystal planes, expressed as a fraction of all crystal planes of that type in the sample, that will diffract into the instrumental aperture at any value of 2θ . A final form of a working equation for quantitative analysis is thus

$$\frac{N_1}{N_2} = \frac{n_1(1 + \cos^2 2\theta_1) \sum_0^{90} e^{-\kappa_2^2 \epsilon^2} \Delta \epsilon \sin 2\theta_2}{n_2(1 + \cos^2 2\theta_2) \sum_0^{90} e^{-\kappa_1^2 \epsilon^2} \Delta \epsilon \sin 2\theta_1}$$

where N_1/N_2 is the ratio of reflecting planes between mineral one and mineral two, and the other quantities θ_1 , θ_2 , κ_1 , κ_2 are similarly identified with the two mineral species. Of course, this equation is only part of the intensity ratio between peaks from two mineral species. Other factors not considered here include appropriate unit-cell transforms, crystallite size, micro-absorption characteristics and other factors which conspire to make quantitative analysis by X-ray diffraction a formidable undertaking.

Results

Calculated results

Figure 4 shows calculated results for the Lorentz factor as a function of orientation (S), and Soller slit spacing (S_0). The results have been normalized to the random-powder Lorentz factor at $50^\circ 2\theta$. Consequently, a value of unity signifies perfect correspondence to the random powder form. Data apply to two commonly encountered clay reflections, namely, the mica 001 at $8.8^\circ 2\theta$ ($\text{CuK}\alpha$ radiation) and the glycol-smectite 001 at $5.2^\circ 2\theta$. At higher diffraction angles, the intensity distribution rapidly approaches the random powder form, but at lower angles larger departures occur.

For a Soller slit spacing of 0.1 cm (General Electric XRD-5 medium resolution slit) the mica 001 gives approximately 90 percent of the intensity predicted by the random powder equation, down to a value of $S \sim \pm 12^\circ$. At $S_0 = 0.05$, essentially random powder characteristics are followed until the orientation is about $\pm 5^\circ$. As expected, the smectite 001 shows greater departures due to its smaller diffraction angle. Errors of 20 percent in intensity will occur if the random powder correction is used for data obtained with the medium resolution Soller slit. If the fine slit is used, random powder characteristics are followed within 10 percent down to $S = \pm 10^\circ$.

Figure 4 shows that the random powder intensity distribution is followed even for well-oriented specimens ($S = \pm 10^\circ$) at error levels of 20 to 30 percent. If fine Soller slits ($S_0 = 0.05$) are employed, the errors are greatly minimized. The single crystal Lorentz factor departs by a factor of approximately ten from the random powder version at the angle of the smectite 001. Consequently the random powder version is the one to apply unless the investigator is willing and able to measure the distribution function for a particular mineral sample, and then to calculate the correct effects by means of the equations presented above. In several publications, Reynolds has stressed the applicability of the random powder form to oriented clay diffraction mounts, and the data of Figure 4 tend to confirm this empirical finding analytically.

The intensity is less than that provided by the random powder Lorentz factor because of two conditions. At low values of S , and low values of 2θ , the slit aperture intercepts many or most of the diffraction rays from the crystallites. Thus diminishing 2θ further causes only a relatively small increase in the number of diffraction rays entering the slit, and the rate of intensity increase with diminishing 2θ is re-

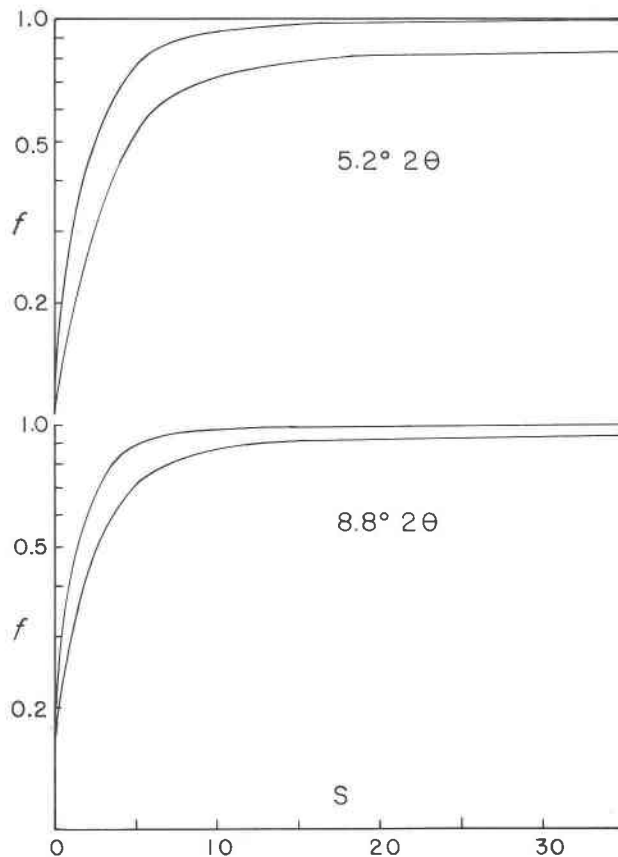


FIG. 4. Lorentz factor at 5.2 and $8.8^\circ 2\theta$ for $S_0 = 0.1$ (lower curves), and $S_0 = 0.05$ (upper curves). The quantity f is the fraction of the random powder value.

duced. At larger values of S and S_0 , that is, on the plateau regions of Figure 4, the diminution of intensities at low 2θ is due to the relative importance of slit-width as opposed to slit-height limitations (Figure 2). This difference, amounting to about 18 percent for the smectite 001 and 8 percent for the mica 001 under the geometric conditions applied here, is a consequence of the assumption that the powder diffraction arcs are very thin compared to the slit-width. If the intrinsic diffraction line breadth is large compared to the width of the slit, or if the sample surface is rough, the diffraction rings will be broad because they are composed of a multiplicity of rings staggered parallel to W (Fig. 2b), and then a rigorous analysis requires summing these in a direction parallel to the slit-width. Under these circumstances, the intensity at low 2θ is no longer strictly slit-width limited, and the lower of each of the two curves in Figure 4a and 4b approaches the upper at moderate to high values of S . That is, line broadening and sample roughness

cause the intensity distribution to move closer to that predicted by the random powder Lorentz factor. The added complication of two more dimensions of summation (one over a Gaussian line-breadth function, and one over a range that extends from the lowest to the highest point on the sample surface) seems hardly worthwhile, providing, as it does, only a small refinement in accuracy, but causing the length of the calculations to press the limits of modern digital computers. It is far simpler to use fine Soller slits in conjunction with the random powder Lorentz factor.

Experimental results

It is difficult to test the accuracy of the formulae derived above. No clay structures are known with sufficient accuracy to allow residual errors in a structural analysis to be assigned solely to the Lorentz factor. For this reason the treatment presented here must be accepted or rejected on the basis of the appropriateness and accuracy of the mathematical approach used. But some confirmation can be obtained by comparing relative intensities of different peaks from a single mineral, obtained with two different Soller slit spacings. The data of Table 1 contain such information. Results were obtained with a G.E. XRD-5 diffractometer, $\text{CuK}\alpha$ radiation, 0.2° detector slit, and utilizing Soller slits with plate spacings of 0.1 cm and 0.05 cm. Table 1 gives measured and calculated values for the change in absolute intensities of the illite 001 and 003, and a glycol-smectite 001 and 005, obtained with the two Soller slit spacings. In addition, data are given (Q) on the increase in the intensity ratio 001/003 (or for smectite, 001/005) caused by the use of the finer (0.05 cm) Soller slit compared to the coarser. The values for S are as-

sumed ones, and of course, can be selected with considerable latitude, because the results are not sensitively related to S if S is indeed above the critical transition value (see Figure 4).

As expected, the use of fine Soller slits causes the intensity ratio to move toward that described by the random powder Lorentz factor (*cf.* Figure 4). In addition, the amount of change (Q), 7 to 18 percent, is consistent with the expected values, calculated for the different slits. In short the assumption of non-extreme values for preferred orientation predicts intensity changes that roughly compare with measured values. The experimental data thus tend, in a small measure, to confirm the calculated results.

The values for the absolute change in peak height with different Soller slits, calculated by means of (6) above, also compare well with experimental values. At $26.6^\circ 2\theta$ most of the integrated powder arcs are of such curvature that they are slit-height limited, consequently doubling the slit-height (Soller slit spacing) causes approximately a doubling of intensity. At lower values of 2θ , however, many more of the arcs are slit-width limited, hence the increase in intensity is less than double. Again, these values tend to confirm the validity of the approach used here. Significantly, the data indicate that standard methods of sample preparation produce degrees of preferred orientation that are insufficiently extreme to cause wide departures from the random powder form of the Lorentz factor.

Discussion and conclusions

Oriented clay specimens produce diffraction profiles that are controlled by a Lorentz factor very close to the random powder form. For all but the most critical work, the investigator will make only small errors if he applies the random powder form. When accurate intensities are crucial, strategies can be formulated that minimize or eliminate possible departures from the random powder Lorentz factor.

For quantitative analysis, higher order reflections should be used whenever possible. Figure 4 shows data only for the mica and smectite 001, but at higher diffraction angles, departures from the random powder form became insignificant for either Soller slit. If low-order reflections must be used, as, for example, in structure determinations, the use of the finest Soller slit is indicated. This will cause an intensity loss of about a factor of two, but intensity is not normally a problem with the low-order reflections. To test for errors caused by very high degrees of preferred orientation, it is useful to generate diffraction patterns

TABLE 1. Intensity data for Soller slit spacings
 $S_0 = 0.1$ and $S_0 = 0.05$

		$I(S_0=0.1)$		Q^*
		$I(S_0=0.05)$		
		Calc.	Obs.	
<2 μ Glycol - smectite Porous plate, S - 20	001	1.65	1.64	18%
	005	2.00	2.00	
<2 μ Illite Glass slide, S - 8	001	1.78	1.78	14%
	003	1.93	2.05	
2-20 μ Muscovite Glass slide, S - 20	001	1.86	1.74	7%
	003	2.00	1.88	
<2 μ Interstratified (Glycol)-Smectite-Illite 10% Smectite, porous plate, S - 8	$9^\circ 2\theta$	1.78	1.69	14%
	$26.7^\circ 2\theta$	1.93	1.93	

* Q is the percent increase in intensity ratio 001/003 or 001/005 observed with $S_0=0.05$ compared to $S_0=0.1$

utilizing different Soller slit spacings. If the two slits produce identical patterns, or if the differences (*e.g.* Q in Table 1) are not greater than that predicted from the plateau values in Figure 4, the investigator can confidently apply the random powder form to the pattern obtained by means of the fine slit.

MacEwan *et al.* (1961) have pointed out that the correct value for oriented aggregates will lie between the two possible forms of Lorentz factor, and that the exact value will depend on the degree of preferred orientation. The analyses presented here show that this view is qualitatively correct, but what is not generally appreciated is the very large degree of preferred orientation necessary to cause significant departures of the Lorentz factor from its random powder form.

References

- JAMES, R. W. (1965) *The Optical Principles of the Diffraction of X-Rays*. Cornell University Press, Ithaca, New York. 664 p.
- MACEWAN, D. M. C., A. RUIZ AMIL AND G. BROWN (1961) Interstratified clay minerals. In, G. Brown, Ed., *The X-Ray Identification and Crystal Structures of Clay Minerals*. Mineralogical Society, London, 544 p.
- REYNOLDS, R. C. (1965) An X-ray study of an ethylene glycol-montmorillonite complex. *Am. Mineral.* **50**, 990-1001.
- (1967) Interstratified clay systems: calculation of the total one-dimensional diffraction function. *Am. Mineral.* **52**, 661-672.
- (1969) Orientation of ethylene glycol monoethyl ether molecules on montmorillonite. *Am. Mineral.* **54**, 562-567.
- AND J. HOWER (1970) The nature of interlayering in mixed-layer illite-montmorillonites. *Clays, Clay Min.* **18**, 25-36.

Manuscript received, June 9, 1975; accepted for publication, January 23, 1976.